Acoustic metamaterials capable of both sound insulation and energy harvesting

OPEN ACCESS
IOP Publishing
Smart Materials and Structures
Smart Mater. Struct. **25** (2016) 045013 (5pp)
doi:10.1088/0964-1726/25/4/045013

Acoustic metamaterials capable of both sound insulation and energy harvesting

Junfei Li[1], Xiaoming Zhou[1], Guoliang Huang[2] and Gengkai Hu[1]

[1] Key Laboratory of Dynamics and Control of Flight Vehicle, Ministry of Education and School of Aerospace Engineering, Beijing Institute of Technology, Beijing 100081, People's Republic of China
[2] Department of Mechanical & Aerospace Engineering, University of Missouri–Columbia, Columbia, MO, USA

E-mail: zhxming@bit.edu.cn and hugeng@bit.edu.cn

Received 22 August 2015, revised 29 December 2015
Accepted for publication 11 January 2016
Published 14 March 2016

Abstract

Membrane-type acoustic metamaterials are well known for low-frequency sound insulation. In this work, by introducing a flexible piezoelectric patch, we propose sound-insulation metamaterials with the ability of energy harvesting from sound waves. The dual functionality of the metamaterial device has been verified by experimental results, which show an over 20 dB sound transmission loss and a maximum energy conversion efficiency up to 15.3% simultaneously. This novel property makes the metamaterial device more suitable for noise control applications.

Keywords: acoustic metamaterials, PVDF membrane, energy harvesting

(Some figures may appear in colour only in the online journal)

1. Introduction

Noise has long been a nuisance for humans. For low-frequency sound insulation, thick and heavy blockage materials have to be used according to the mass density law. Hence, a thin and light-weight insulation material that can break the mass law is of great interest for noise control. In recent years, the development of acoustic metamaterials has provided a promising direction for low-frequency sound insulation [1–8]. Based on the local resonance mechanism, acoustic metamaterials achieve sound insulation in the form of total reflection. As an example, membrane-type acoustic metamaterials are composed of a thin membrane with one or multiple rigid masses attached to the membrane. Compared with ordinary insulation materials, they can exhibit very strong acoustic attenuation in a deep sub-wavelength distance [5, 13–23]. From a practical point of view, sound insulation and energy retrieved from these noises are compatible and should be preferable. The realization of this dual functionality is possible since the structure resonance usually causes the enhancement and localization of the deformation energy, which can be readily retrieved with energy conversion devices.

Advances in the structure-borne sound regime have been achieved regarding this issue. Gonella *et al* [9] introduced piezoelectric cantilevers into a solid lattice structure to harvest energy within the band gap. Carrara *et al* [10] used a parabolic acoustic mirror (PAM) to focus the structure-borne wave energy and harvested the energy localized in the region of imperfection in aluminum stubs. Mikoshiba *et al* [11] used an array of resonators to harvest energy with electromagnetic induction. Ahmed *et al* [12] embedded piezoelectric wafers in the soft matrix of an acoustic metamaterial and achieved a dual mode of acoustic filter and an energy harvester simultaneously.

Regarding the dual functionality of membrane-type acoustic metamaterials, Ma *et al* have made a first attempt at the simultaneous control of acoustic absorption and energy harvesting, with the latter mechanism based on electromagnetic induction [22]. In this work, we focus on sound isolation and energy harvesting based on piezoelectric

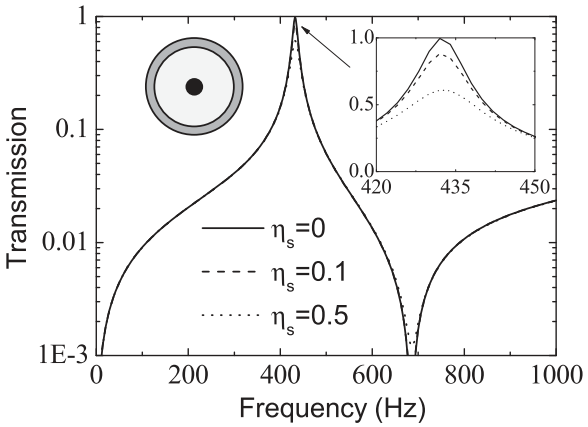

Figure 1. Acoustic transmission of the membrane-type metamaterial in the case of different loss tangent $\eta_s = 0$, 0.1, and 0.5.

materials. The design and evaluation of this metamaterial device will be studied by both numerical and experimental methods.

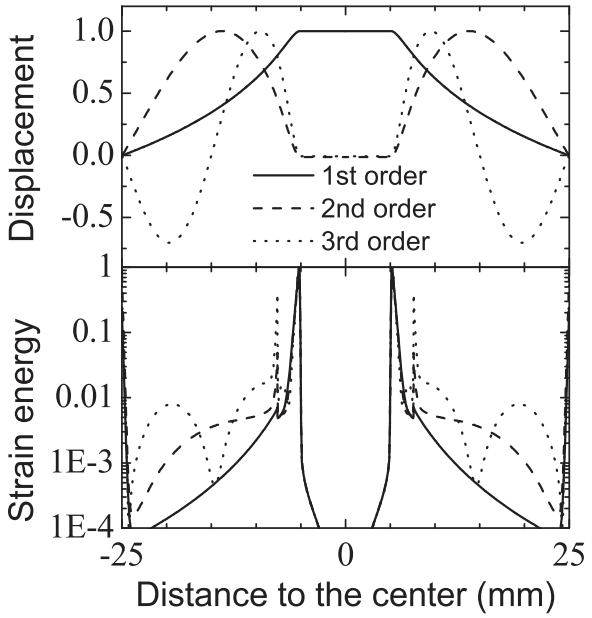

Figure 2. First three-order mode shapes of displacement and strain energy along the central line of the membrane structure.

2. Design of the device

The basic structure of the device consists of a pre-stretched thermoplastic polyurethane (TPU) circular membrane with a diameter of 50 mm and a thickness of 0.07 mm. The boundary of the membrane is fixed by a rigid aluminum ring, and two aluminum sheets with a diameter of 10 mm and a thickness of 2 mm are attached to the center of both sides of the membrane. Young's modulus, Poisson's ratio and the mass density of the TPU are respectively $3(1 + \eta_s)$ GPa, 0.38, and $1250\,\mathrm{kg/m^3}$, where η_s is the loss tangent. Numerical simulation results of the normal-incidence transmission coefficient of the structure are shown in figure 1 in the case of the pre-stress 64.3 MPa for the membrane. This model structure, first proposed by Yang *et al,* is termed as membrane-type acoustic metamaterial, and is well known for sound insulation due to the negative mass density between the resonance frequency 432 Hz and anti-resonance frequency 684 Hz. In the absence of the membrane loss $\eta_s = 0$, the sound insulation is least effective around the resonant frequency 432 Hz where complete acoustic transmission can be achieved. When the membrane loss is introduced, the transmission loss near such a frequency can be significantly enhanced due to energy dissipation in the membranes. As a result, high transmission loss in a broad band can be obtained without the defection near the resonant frequency. The purpose of this work is to retrieve this part of the energy, instead of having it dissipate, and to propose a metamaterial device capable of both sound insulation and energy harvesting.

Figure 2 shows the displacement and strain energy distribution in the line across the center of the membrane at the first three-order resonant frequencies of the membrane structure. It can be observed that the strain energy of the bending deformation is greatest in the perimeter region of the central

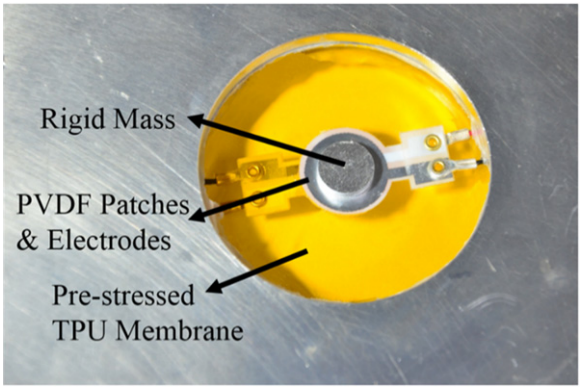

Figure 3. The proposed metamaterial device.

mass. In the membrane loss case, the strain energy in this region will intensively dissipate, as a result of the enhanced transmission loss near the resonant frequency. Our idea is to harvest this part of the strain energy with flexible PVDF piezoelectric materials. To this end, PVDF materials with an outer diameter of 15 mm and a thickness of 0.05 mm are attached on both sides of the membrane and encircling the central mass, as shown in figure 3. Rather than the hard PZT material with the higher conversion efficiency, the Flexible PVDF is used here to avoid the alteration of the mode shape of the membrane structure.

As a theoretical explanation, assume that the added PVDF membrane has a negligible effect on the vibration of the TPU membrane. We can obtain the membrane's displacement by numerical simulation in response to incident acoustic waves at first. Then, the deformation of the piezoelectric membrane can be evaluated with the Lagrange–Green

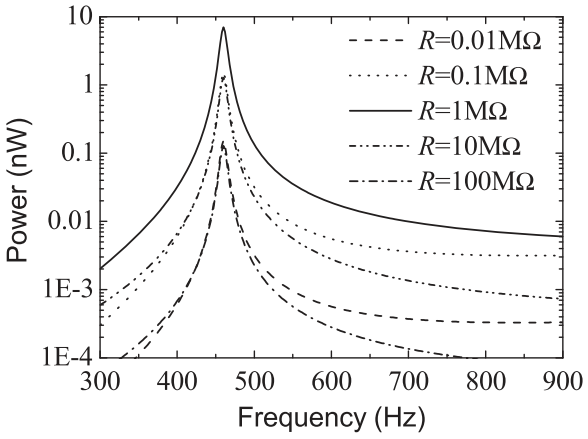

Figure 4. Energy dissipation by the resistors with different values of R.

strain tensor $\mathbf{S}$

$$\mathbf{S} = \frac{1}{2}[\mathbf{u}\nabla + \nabla\mathbf{u} + \nabla\mathbf{u}\cdot\mathbf{u}\nabla] \tag{1}$$

Considering the thickness-polarized piezoelectric state, the electric displacement is given by

$$\mathbf{D} = \mathbf{eS} + \varepsilon\mathbf{E} \tag{2}$$

where $\mathbf{E}$, ε, and $\mathbf{e}$ are respectively the electric field, permittivity and piezoelectric stress constant. The electric charge output can be calculated using Gauss's law [19, 20]

$$Q(t) = \iint_{S_e} D_3 \mathrm{d}x\mathrm{d}y \tag{3}$$

where S_e is the area covered by the electrode on the PVDF membrane. The voltage output is $U = Q/C$ where the capacitance is $C = \varepsilon S_e/h$, and h is the thickness of the piezoelectric material. We define the local voltage

$$U_{\mathrm{local}} = \frac{hD_3}{\varepsilon} \tag{4}$$

and substitute it into equation (3) to get the voltage output

$$U = \frac{1}{S_e}\iint U_{\mathrm{local}}\,\mathrm{d}x\mathrm{d}y \tag{5}$$

The result shows that the net voltage output is the averaging of the local voltage. This confirms that the PVDF film should be attached onto those regions with high strain energy.

For numerical verification of acoustic energy harvesting, numerical simulations are conducted based on Acoustic-Piezoelectric Interaction Modulus of COMSOL Multiphysics. Two PVDF patches are loaded with identical resistors R. The energy dissipated by the resistor can represent the energy harvesting capacity of the device. Figure 4 shows the energy dissipation in the case of five different resistor values. It can be seen that the energy output in the case of 10 MΩ is greater than those in other cases. The reason is that the PVDF patch behaves as a capacitor and the external circuit is a pure resistor. The maximum harvested energy output, in this case, is as a result of the impedance matching between the terminated circuit and the PVDF patch [24].

3. Experimental results

In the experiment, a TPU membrane with a thickness of 0.07 mm is used. The procedure to apply the pre-stress on the membrane is as follows. The membrane is covered on one side of a hollow aluminum cylinder with the other side enclosed. The air pressure in the cylinder is enhanced with a pump and the pressure value is accurately tuned by an E/P Converter. The pre-stress in the membrane can be calculated from the known air pressure in the cylinder. Then a rigid circular ring is stuck onto the stretched membrane. After a few hours, the pressure vessel can be deflated and a membrane with uniform pre-stress is obtained. The TPU membranes with two different pre-stresses of 64.3 and 42.0 MPa are fabricated. For each sample, two circular PVDF patches with an outer diameter of 15 mm are attached to the center of both sides of the membrane. Two identical aluminum cylinders with a diameter of 10 mm and a thickness of 2 mm are glued onto the membrane, acting as the central mass. Each PVDF patch is loaded with a resistor of 1 MΩ. Acoustic scatterings of the sample are measured with a B&K 4206T impedance tube. The voltage output from the PVDF patch is measured with a National Instrument USB-6356 DAQ system. The configuration of the measurement system is shown in figure 5.

Figure 6 shows the energy transmission, reflection, and absorption spectra of two metamaterial samples. Transmission and absorption in the case of the membrane stress of 64.3 and 42.0 MPa reach their maximum values at the sample's first resonant frequencies of 432 and 356 Hz, respectively. The absorption peaks are almost up to 0.5, which can be attributed to the energy-harvesting capability of the device, as verified in figure 7, where the corresponding peaks of the voltage output can be clearly observed. The above experimental results have demonstrated that the proposed metamaterial devices can not only block sound waves with over 20 dB STL, but harvest acoustic energy using the membrane's resonant behavior. This dual functionality is desirable for noise control.

Finally, we attempt to evaluate the energy conversion efficiency of the metamaterial device. Here, the energy conversion efficiency c is defined to be the ratio of the output electrical power W_e and input acoustic power W_a, and given by

$$c = \frac{W_e}{W_a} = \frac{2U_e{}^2/R}{S_m p_e{}^2/\rho_0 c_0{}^2} \tag{6}$$

where U_e is the output voltage of the PVDF patches, $\rho_0 c_0{}^2 = 1.5464 \times 10^5$, and S_m is the cross-section area of the impedance tube. Figure 8 shows the energy conversion efficiency as a function of frequency. It can be seen that the maximum efficiencies of 15.3 and 10.3% are obtained for both samples. The results make the proposed device a potential candidate for energy harvesting in noise environments.

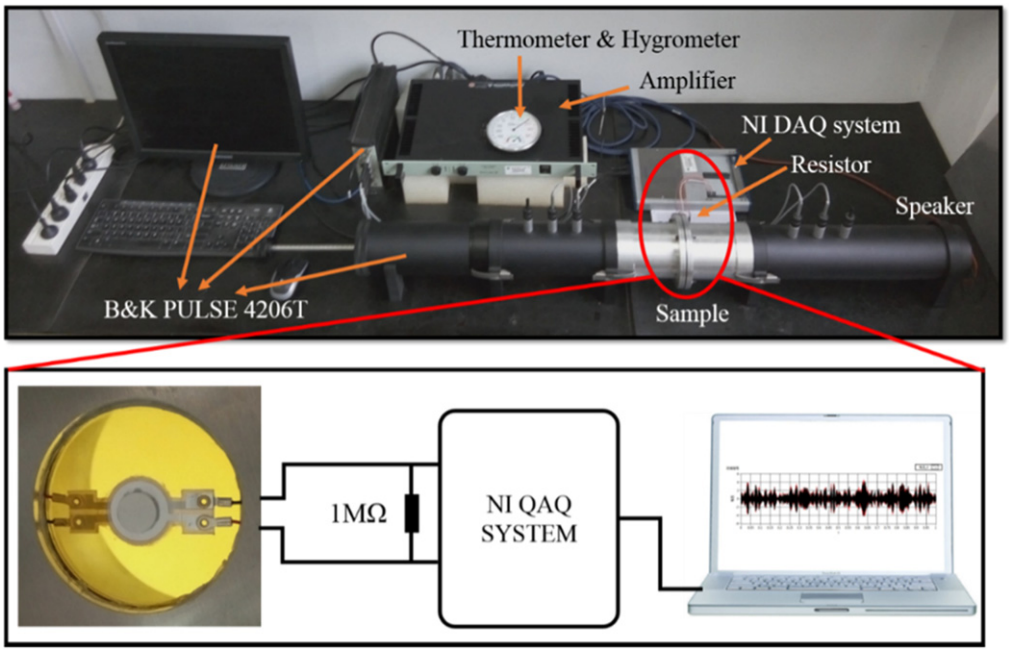

Figure 5. Configuration of the metamaterial device and measurement system.

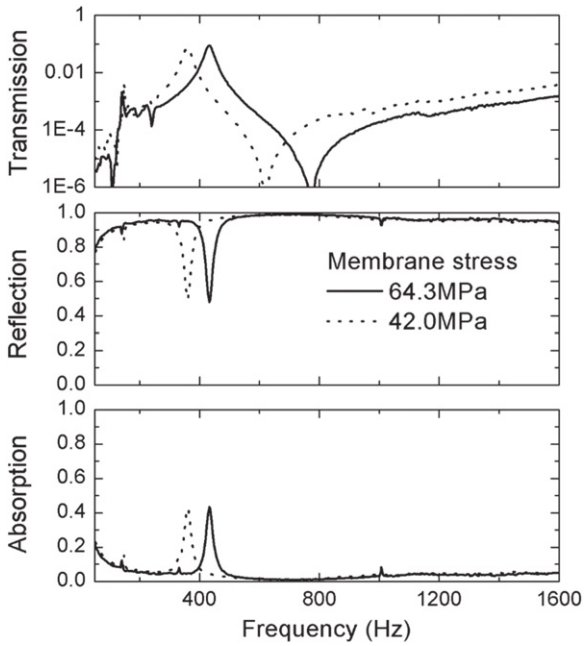

Figure 6. Energy transmission, reflection, and absorption spectra of the metamaterial device with different membrane stresses of 64.3 and 42.0 MPa.

We would like to emphasize that the structure considered in this work is different from the structure reported by Ma *et al* [22]. In our model, the membrane is arranged in an infinite air background. However, the membrane encloses an air cavity in Ma's structure [22]. This difference in their model geometry results in a big difference in their acoustic absorption ability. For the membrane model without the enclosed cavity, like ours, we have demonstrated in theory

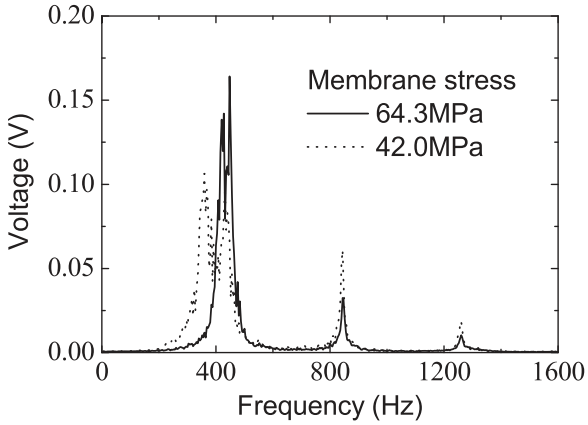

Figure 7. The output voltage from the metamaterial devices.

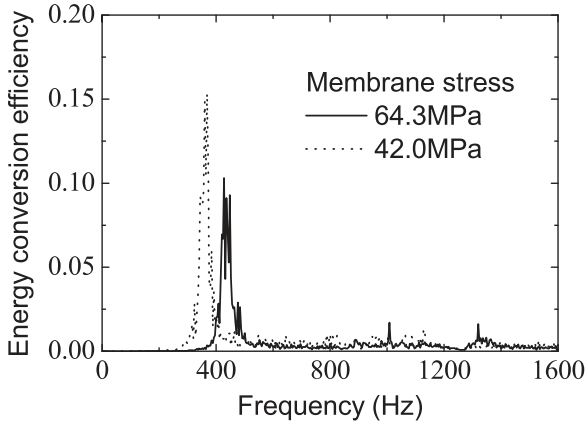

Figure 8. Energy conversion efficiency of the metamaterial device with different membrane stresses of 64.3 and 42.0 MPa.

that the upper limit of their acoustic absorption is half of the incident power, whatever the values of the losses of the membranes are [17]. This limit always exists as long as the continuous velocity condition across the membrane exists. While for Ma's structure [22], the continuous condition does not exist, so their absorption coefficient can be unity. The idea of energy harvesting is to harvest the energy that should have been absorbed by the membrane. As a result of the difference in the absorption limit, the maximum sound energy-harvesting efficiency of 15.3% for ours is lower than in Ma's structure (23%) [22]. But this does not mean that the proposed model is inferior.

4. Conclusions

We have proposed a novel metamaterial device capable of both sound insulation and energy harvesting. The proposed device exhibits a substantial sound insulation ability, STL over 20 dB below 1.6 kHz, and is able to convert acoustic energy into electric energy with the maximum conversion efficiency up to 15.3% near the resonant frequency 356 Hz of the metamaterial. These novel properties make the metamaterial devices suitable for use in loud noise environments such as airports, highways, and factories, etc.

Acknowledgments

The authors would like to thank Liu Xiaoning and Zhang Yidan for helpful discussions. This work is supported by NSFC through Grants 11521062, 11290153 and 11572039.

References

[1] Liu Z, Zhang X, Mao Y, Zhu Y Y, Yang Z, Chan C T and Sheng P 2000 Locally resonant sonic materials *Science* **289** 1734–6
[2] Fang N, Xi D, Xu J, Ambati M, Srituravanich W, Sun C and Zhang X 2006 Ultrasonic metamaterials with negative modulus *Nat. Mater.* **5** 452–6
[3] Huang H H, Sun C T and Huang G L 2009 On the negative effective mass density in acoustic metamaterials *Int. J. Eng. Sci.* **47** 610–7
[4] Yao S, Zhou X and Hu G 2008 Experimental study on negative effective mass in a 1D mass–spring system *New J. Phys.* **10** 043020
[5] Yang Z, Mei J, Yang M, Chan N H and Sheng P 2008 Membrane-type acoustic metamaterial with negative dynamic mass *Phys. Rev. Lett.* **101** 204301
[6] Lee S H, Park C M, Seo Y M, Wang Z G and Kim C K 2009 Acoustic metamaterial with negative density *Physics Letters A* **373** 4464–9
[7] Lee S H, Park C M, Seo Y M, Wang Z G and Kim C K 2009 Acoustic metamaterial with negative modulus *J. Phys.: Condens. Matter.* **21** 175704
[8] Fok L, Ambati M and Zhang X 2008 Acoustic metamaterials *MRS Bull.* **33** 931–4
[9] Gonella S, To A C and Liu W K 2009 Interplay between phononic bandgaps and piezoelectric microstructures for energy harvesting *J. Mech. Phys. Solids* **57** 621–33
[10] Carrara M, Cacan M R, Toussaint J, Leamy M J, Ruzzene M and Erturk A 2013 Metamaterial-inspired structures and concepts for elastoacoustic wave energy harvesting *Smart Mater. Struct.* **22** 065004
[11] Mikoshiba K, Manimala J M and Sun C T 2013 Energy harvesting using an array of multifunctional resonators *J. Intell. Mater. Syst. Struct.* **24** 168–79
[12] Ahmed R U and Banerjee S 2014 Low frequency energy scavenging using sub-wave length scale acousto-elastic metamaterial *AIP Advances* **4** 117114
[13] Yang Z, Dai H M, Chan N H, Ma G C and Sheng P 2010 Acoustic metamaterial panels for sound attenuation in the 50–1000 Hz regime *Appl. Phys. Lett.* **96** 041906
[14] Naify C J, Chang C M, McKnight G, Scheulen F and Nutt S 2011 Membrane-type metamaterials: transmission loss of multi-celled arrays *J. Appl. Phys.* **109** 104902
[15] Mei J, Ma G, Yang M, Yang Z, Wen W and Sheng P 2012 Dark acoustic metamaterials as super absorbers for low-frequency sound *Nat. Commun.* **3** 756
[16] Chen Y, Huang G, Zhou X, Hu G and Sun C T 2014 Analytical coupled vibroacoustic modeling of membrane-type acoustic metamaterials: membrane model *J. Acoust. Soc. Am.* **136** 969–79
[17] Chen Y, Huang G, Zhou X, Hu G and Sun C T 2014 Analytical coupled vibroacoustic modeling of membrane-type acoustic metamaterials: plate model *J. Acoust. Soc. Am.* **136** 2926–34
[18] Naify C J, Chang C M, McKnight G and Nutt S 2011 Transmission loss of membrane-type acoustic metamaterials with coaxial ring masses *J. Appl. Phys.* **110** 124903
[19] Xiao S, Ma G, Li Y, Yang Z and Sheng P 2015 Active control of membrane-type acoustic metamaterial by electric field *Appl. Phys. Lett.* **106** 091904
[20] Ma F, Wu J H and Huang M 2015 Resonant modal group theory of membrane-type acoustical metamaterials for low-frequency sound attenuation *Eur. Phys. J. Appl. Phys.* **71** 30504
[21] Yang M, Ma G, Yang Z and Sheng P 2013 Coupled membranes with doubly negative mass density and bulk modulus *Phys. Rev. Lett.* **110** 134301
[22] Ma G, Yang M, Xiao S, Yang Z and Sheng P 2014 Acoustic metasurface with hybrid resonances *Nat. Mater.* **13** 873–8
[23] Yang M, Li Y, Meng C, Fu C, Mei J, Yang Z and Sheng P 2015 Sound absorption by subwavelength membrane structures: a geometric perspective *Comptes Rendus Mécanique* **343** 635–44
[24] Høgsberg J and Krenk S 2015 Balanced calibration of resonant piezoelectric RL shunts with quasi-static background flexibility correction *J. Sound Vib.* **341** 16–30